International Journal on Magnetic Particle Imaging
Vol 9, No 1, Suppl 1, Article ID 2303030, 5 Pages

Proceedings Article

Highly flexible gradiometer coil arrangement offering improved passive compensation for multi-frequency MPI

H. Radermacher[a,*] · F. Schrank[a] · D. Pantke[a] · F. Mueller[a] · M. Peters[a] · V. Schulz[a,b,c,d,*]

[a]Department of Physics of Molecular Imaging Systems, Institute for Experimental Molecular Imaging, RWTH Aachen University, Aachen, Germany
[b]Hyperion Hybrid Imaging Systems GmbH, Pauwelsstrasse 19, 52074 Aachen, Germany
[c]III. Physikalisches Institut B, Otto-Blumenthal-Strasse, 52074 Aachen, Germany
[d]Fraunhofer Institute for Digital Medicine MEVIS, Forckenbeckstrasse 55, Aachen, Germany
*Corresponding author, email: harald.radermacher@pmi.rwth-aachen.de, volkmar.schulz@pmi.rwth-aachen.de

Abstract

In Magnetic Particle Imaging (MPI), the acquired receive signal will contain both the superparamagnetic iron oxide nanoparticle (SPION) signal as well as the excitation signal, where the former is to be maximized while the latter is to be reduced. Gradiometer receive coils can offer such reduction. Effective suppression of excitation feedthrough requires various degrees of freedom (DOF) for adjusting geometrical positions, amplitudes, etc. In this work, a suitable MPI coil arrangement is presented. The adjustment process is based on the signals acquired by the receive chain and can be fully automated. The coil arrangement is realized as a scanner with a diameter of approximately 34 mm; one dimension is scanned electrically while full three dimensional scanning can be achieved via the mechanical DOFs by means of a robotic stage. Electrical characterization shows passive feedthrough suppression of more than 100 dB at fundamental frequency. First measurements of SPION samples are presented.

I. Introduction

Magnetic particle imaging is based on generation of magnetic excitation fields and sensing the response of SPIONs, exposed to this field, at selected locations. It is of key importance to limit feedthrough, i.e., the receive signal that originates from the excitation field signals in the transmit coil.

Using fixed frequency sinusoidal excitation, the effect of feedthrough can be minimized via analog filtering and digital signal processing [1], by suppressing the excitation frequency and focusing on the higher order harmonics, generated by the (de-)saturation of the magnetic particles. However, information in the fundamental frequency response of the SPIONs is lost, too. When interested in information on the temperature or viscosity of the medium, comprising the SPIONs, one way is to perform multiple measurements at different excitation frequencies. While generating these frequencies is easy to accomplish, the creation of multiple high current drive signal filters and matching filters for the receive signal would result in increased hardware effort. Hence, in such cases, effective suppression of feedthrough directly at coil level can be applied [1, 2]. Theoretically, full compensation of the feedthrough would be possible [3], however practical results are typically limited in the range of 60 dB to 82 dB suppression [1, 2, 4, 5]. Imperfect symmetry of the coil arrangement, the magnetic field of

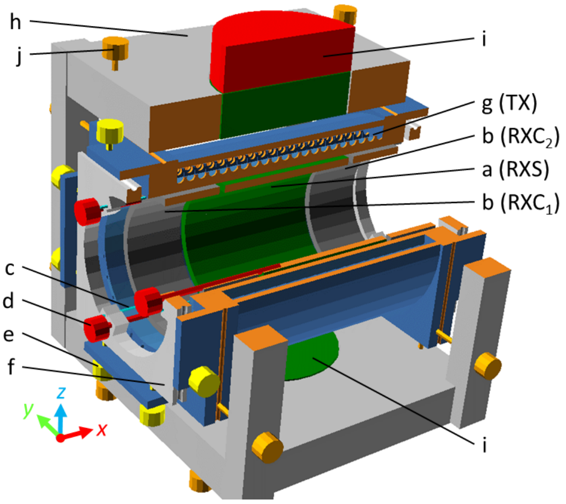

Figure 1: Rendering of MPI Scanner. Receive coil carriers RXS (green, a) and RXC$_n$ (grey, b), guided by support rods (cyan, c) can be translated by threaded rods (red, d). Position of this receive module is determined by screws (yellow, e) holdings its adapter plate (light grey, f) with respect to the transmit coil carrier (blue, g). Surrounding frame (grey, h) holding the selection field magnets (i) can be adjusted wrt. the transmit coil via screws (orange, j).

wires for connecting the transmit coil, capacitive coupling, loading by a single-ended receive amplifier, etc. are factors contributing to this.

I.I. Aim

In this work, a coil arrangement with flexible positioning is presented, offering a high number of DOF to align the geometrical positions and to set amplitude and phase of the signals with respect to each other for achieving significant improvement in passive compensation compared to previous work [2]. A gradiometer design is used for the receive coil. The transmit coil is a simple solenoid without compensation windings, reducing the number of turns and hence inductance of the transmit coil compared to [2], resulting in lower required drive voltage.

I.II. Influence factors for compensation signals

The set of coils in an MPI Scanner can, in the simplest case, be seen as a weakly coupled transformer, where the two compensation windings (RXC$_1$, RXC$_2$) exhibit reversed polarity compared to the sense winding (RXS). For perfect compensation, the received signal has to fulfil

$$U_{\mathrm{RXC1}} + U_{\mathrm{RXC2}} + U_{\mathrm{RXS}} = 0 \quad (1)$$

in response to the time derivative of the magnetic flux generated by the transmit coil (TX). The compensation signal voltage can be set by adjusting the final position of the coils RXC$_n$ in the expanding drive field towards the ends of the transmit coil. Therefore, the coils are to be moved in x-direction, while y- and z-positions are kept stable.

The transmit coil has to be equipped with feeding wires for connection to the power amplifier, which are generating magnetic fields, too. The magnetic x-axis location will hence divert from the geometric axis of the coil carrier; the axes may not even be parallel to each other. Same has to be expected for the magnets generating the field free point (FFP).

The MPI scanner was, hence, designed (Fig. 1) such that all elements can be positioned and aligned with respect to each other by multiple sets of screws and threaded rods. This allows for both easy adjustability and sufficient stability against unintended drift. Translational shift and rotation along the x-, y-, and z-axis can be set. The inner section of the coil carrier is shaped as a rounded triangle, maximizing the free volume to allow for in-vivo mice measurements. For sustained operation at the designed peak drive field amplitude of 10 mT, water cooling of the transmit coil is possible in such a way, that all outer surfaces are kept at cooling medium temperature (aiming for 20°C to avoid condensation), preventing heat radiation or convection to both selection field magnets as well as receive coils and sample. The temperature of the transmit coil carrier will be held stable by the water cooling, too. The winding pitch of the transmit coil is firmly set by its carrier. In total, drift due to thermal expansion is minimized.

II. Material and methods

The scanner was constructed in *SOLIDWORKS*® and machined from PVC and acrylic glass. The transmit coil winding support, setting the pitch, is a 3D printed structure made of ASA, glued onto the inner tube. The receive coil support rods as well as the threaded rods for positioning these coils are made from brass, later to be replaced by ceramic and nylon, respectively. *PACK* RUPALIT 13000*0.02 mm and 2300*0.02 mm is used for transmit and receive coils, respectively. Different to a final realization, where extra cable length will be minimized, each of the three sections of the receive coil is fed to the outside, such that U_{RXS}, U_{RXC1} and U_{RXC2} can be accessed individually. The permanent magnets for creating the selection field are wrapped in several layers of 150 µm copper foil.

For the measurements, different setups were used. During electrical testing and tuning, the passive decoupling was determined. The transmit coil was excited with a sinusoidal voltage signal, $f = 10$ kHz, generated by a *Keysight* 33512B, amplified by an *Omnitronic* P-1000 audio amplifier, resulting in an effective excitation voltage of 2.43 V. The signals of the three receive coil sections are

10.18416/ijmpi.2023.2303030

captured individually as well as in series connection by means of a *Tektronix* DPO 4104 oscilloscope. The signal of the center receive coil RXS is recorded as a reference, such that the true feedthrough suppression due to the compensation can be calculated.

Via the various degrees of freedom, the system was set into compensated state: Starting from a symmetrically aligned system, the cancelation coils and the complete receive module where moved iteratively while monitoring the compensated receive voltage. The oscilloscope input sensitivity alone would not allow for accurate measurement in this state, hence the receive signal is amplified by a *Stanford Research Systems* SR560 low-noise amplifier (LNA), set to a gain of 500 for all subsequent measurements. The coupling to the copper wrapped magnets created a phase difference between the voltages in the sense coil and the compensation coils. This was solved by fine positioning of the magnet holder frame. This adjustment impacts the location of the FFP and will need to be reflected in the path of the robot.

For particle measurements, the very same frequency generator in combination with an *AE TECHRON* 7796 power amplifier is used. Isocenter magnetic drive field strength is measured by *F.W. BELL* 5180 Gauss/Tesla Meter. Samples of SHP20 (*Ocean NanoTech LLC*, San Diego, USA) with an iron concentration of 5 mg/ml and C2 [6], 10 mg/ml, were produced. 10 µl of the tracers was diluted in water and glycerol to a total volume of 100 µl, each. These samples are positioned along the x-axis via a 3-axis robot, (*isel*, Dermbach, Germany). The proprietary control system, created in [2], applying active compensation, too, was used to control the setup and to generate and capture the signals.

To test applicability, system matrices were acquired with both C2 and SHP20 samples, measured at 10 kHz with 8 mT peak. The scanned field of view (FOV) of the system matrices is 20 mm with a step size of 1 mm. Directly before and after the system matrix sweeps, five background measurements were acquired and for each system matrix position two averages were used. The background measurements are averaged and subtracted from all particle measurements. For the signal-to-noise ratio (SNR), the particle measurements are scaled to the standard deviation of the background measurements.

III. Results and discussion

The realized scanner is shown in Fig. 2. So far, measurements have been performed without shielding from external distortion. For the phantom measurements, drive field was activated in bursts of 10 ms with a duty cycle of ∼1 %. Acquisition of the mentioned system matrix took approximately 2 minutes, during which the scanner was operated without the outer shell of the transmit coils, so without water cooling. The final, water cooled version will allow for longer scans and higher duty cycle operation.

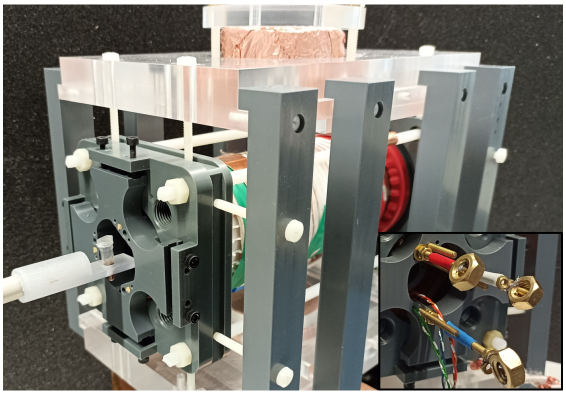

Figure 2: The realized MPI Scanner, a sample is visible outside of the bore. The inset shows the threaded rods for positioning the three receive coil segments along the x-axis as well as their individual twisted pair cables.

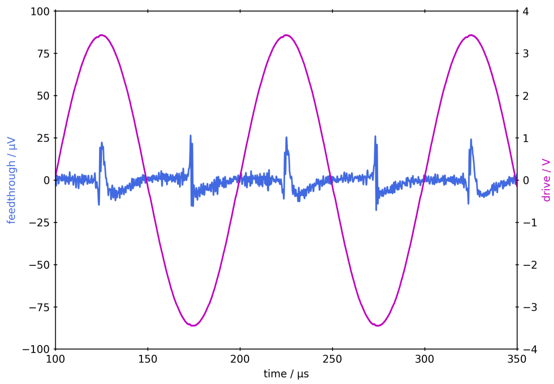

Figure 3: Transmit coil signal (drive, purple, only used as trigger source) and passively compensated receive signal (feedthrough, blue, scaled according to the gain of the LNA). Without compensation, the receive signal would have an effective voltage of 660 mV. Here, the effective voltage is 7.5 µV, which is mainly due to higher order noise, i.e. distortions of the transmit amplifier near the peak of the drive signal.

During electrical testing and tuning, the reference receive signal strength of the center coil alone is determined to be $U_{RXS} = 660$ mV, equivalent to -3.6 dBV. With full alignment and compensation, feedthrough signal is reduced to µV-level, see Fig. 3. Via fast Fourier transform (FFT), the fundamental component is derived to be -117 dBV, equivalent to 1.4 µV, see Fig. 4. Compared to the uncompensated signal of RXS, (-3.6 dBV), fundamental frequency attenuated by 113.4 dB.

As visible in Fig. 3, the distortions in the drive signal around the positive and negative peak create a relatively stronger receive signal, so attenuation for higher harmonics does not reach such high levels. Aiming at multi-frequency MPI, operation at different excitation frequencies is required. Switching of the frequency ini-

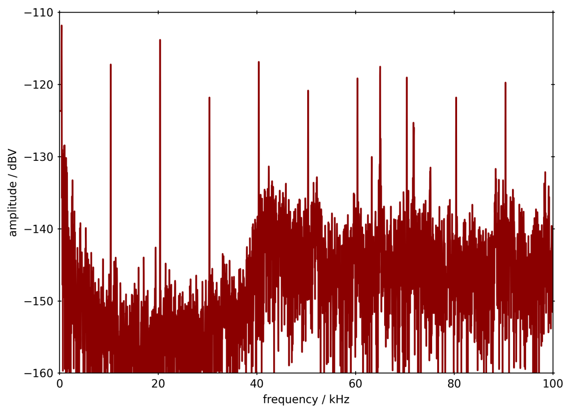

Figure 4: FFT (red) of the passively compensated receive signal. The 10 kHz component is at -117 dBV. This value has to be seen relative to the uncompensated signal of -3.6 dBV. Next to the harmonics of the drive signal, there is also broadband noise. Besides the noise of the receive coil wire resistance and the LNA, this can also be explained by the lack of shielding against external electromagnetic fields.

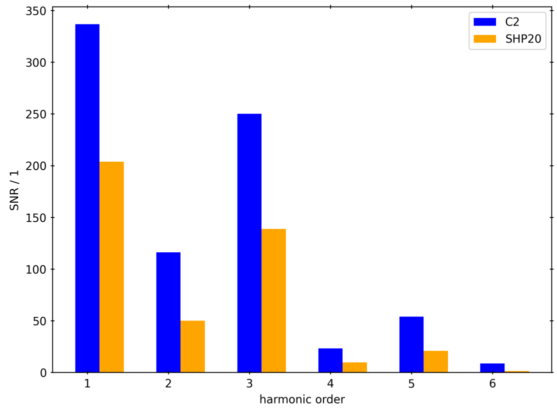

Figure 5: SNRs from C2 (blue) and SHP20 (orange) samples. C2 shows consistently higher SNR than SHP20, due to the higher iron concentration. The fundamental harmonic is visible but relatively small due to a high noise level. Even harmonics are present because the samples where not positioned exactly in the center of the FOV.

tially results in non-optimal attenuation. However, the scanner can be re-tuned easily. To test this, the system was briefly adjusted at frequencies of 5 kHz, 15 kHz, and 25 kHz, too, yielding suppression of the specific fundamental frequency component of at least 110dB in each case. During further investigation, settings for supporting at least two predefined frequencies and/or an automated tuning procedure will be worked out.

The measurements of both C2 and SHP20 samples closest to the FOV's center are used to calculate SNRs which can be seen in Fig. 5. Although very limited statistics is available with two averages, six higher harmonics of both particle samples can be distinguished, including the fundamental harmonic.

Even harmonics are visible due to an imperfect positioning of the samples. However, signal and, hence, SNR is consistently higher for C2, matching the higher iron concentration, which gives first evidence of a proper operation of the scanner. The SNR of the fundamental harmonic is relatively small, which is due to a high noise level, showing that our system is not completely stable yet. Further investigations concerning the stability and the influence thereon from proper shielding and water cooling are left to future work.

The complete background corrected system matrices for both C2 and SHP20 are shown in Fig. 6, scaled to the fundamental harmonic of the center position of C2. Both system matrices show the expected characteristic pattern, especially including the fundamental component. They also show only little noise, but this is expected due to the high iron mass.

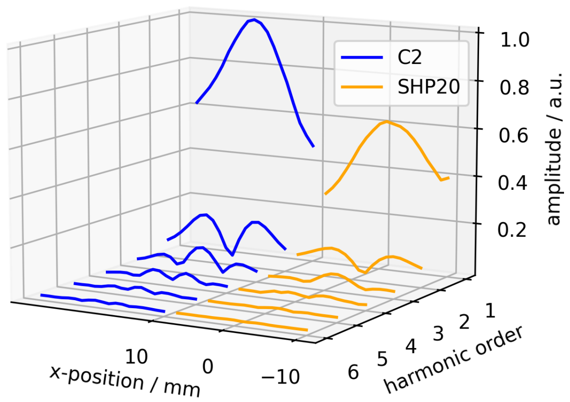

Figure 6: System matrix plot of C2 and SHP20 samples, normalized to the 1^{st} harmonics of C2 along a FOV of 20 mm. Reduced signal from SHP20 is expected, due to lower particle concentration.

IV. Conclusions

An MPI scanner gradiometer coil arrangement can provide >100 dB passive feedthrough suppression of the fundamental frequency, significantly improving the previous achieved results, and is still compatible with additional active compensation. First particle sample scans prove the applicability and look promising; the quantification of sensitivity and resolution gain is pending. In the next phase, shielding and water cooling will be applied, such that this improvement can be further leveraged towards higher LNA gain for better sensitivity as well as longer measurement bursts. Adjustment to different frequencies is possible with the current setup; a version for supporting true multi-frequency MPI without user interaction is planned.

10.18416/ijmpi.2023.2303030

Acknowledgments

We thank the team of the scientific workshop of the University Hospital RWTH Aachen for realizing the mechanical components.We thank Pauline Kreft for the preparation of the SPION samples.Research funding: We acknowledge the financial support by the German research foundation (DFG, grant number SCHU 2973/5-1).

Author's statement

Conflict of interest: Authors state no conflict of interest.

References

[1] M. Graeser, T. Knopp, M. Gruettner, T. Sattel, T. Buzug. Analog receive signal processing for magnetic particle imaging, Med.Phys., 40 (4), 042303, 2013, doi: 10.1118/1.4794482

[2] D. Pantke, N. Holle, A. Mogarkar, M. Straub, and V. Schulz. Multi-frequency magnetic particle imaging enabled by a combined passive and active drive field feed-through compensation approach, Medical Physics, vol. 46, no. 9, pp. 4077–4086, Jul. 2019.

[3] Q. Huynh, B. Fung, C. Saayujya. Design of a more easily shimmable gradiometric coil using linear programming, International Journal on Magnetic Particle Imaging, Vol. 8, no. 1 Suppl 1 , 2022, doi: 10.18416/IJMPI.2022.2203074

[4] A. Cagil, B. Tasdelen, and E. Saritas. Design of a doubly tunable gradiometer coil. International Journal on Magnetic Particle Imaging, 6(2):1–3, 2020, doi:10.18416/IJMPI.2020.2009064.

[5] M. Graeser, T. Knopp, P. Szwargulski, et al. Towards picogram detection of superparamagnetic iron-oxide particles using a gradiometric receive coil. Sci Rep. 2017;7:1–13.

[6] S.M. Dadfar, D. Camozzi, M. Darguzyte, et al. Size-isolation of superparamagnetic iron oxide nanoparticles improves MRI, MPI and hyperthermia performance. J Nanobiotechnol 18, 22 (2020). doi: 10.1186/s12951-020-0580-1

